Sensors and Actuators B 222 (2016) 106–111

Contents lists available at ScienceDirect

Sensors and Actuators B: Chemical

journal homepage: www.elsevier.com/locate/snb

Clam-inspired nanoparticle immobilization method using adhesive tape as microchip substrate

Xiaowen Huang[a,b], Yujiao Zhu[a,b], Xuming Zhang[a,b,*], Zhiyong Bao[b], Dang Yuan Lei[b], Weixing Yu[c], Jiyan Dai[b], Yu Wang[b]

[a] The Hong Kong Polytechnic University Shenzhen Research Institute, Shenzhen, PR China
[b] Department of Applied Physics, The Hong Kong Polytechnic University, Hong Kong SAR, PR China
[c] State Key Laboratory of Applied Optics, Changchun Institute of Optics, Fine Mechanics and Physics, Chinese Academy of Sciences, Chang Chun, PR China

ARTICLE INFO

Article history:
Received 1 June 2015
Received in revised form 31 July 2015
Accepted 15 August 2015
Available online 18 August 2015

Keywords:
Microfluidics
Biomimetics
SERS
Nanoparticle immobilization
Biochip
Microfabrication

ABSTRACT

Immobilization of the suspended nanoparticles is essential for many microfluidic applications. This work reports a novel biomimetic method to immobilize nanoparticles by using a common adhesive tape as the substrate of microfluidic chip. It mimics the clams' feeding system that utilizes the mucus (i.e., sticky fluid) to capture small phytoplankton particles in water. This work proves experimentally that this method has a better immobilization effect and a stronger shear stress resistance than the traditional methods using hard glass substrates. Moreover, we have applied this method to immobilize Au nanorods for the detection of R6G of various concentrations using the surface-enhanced Raman scattering (SERS) effect. This method enjoys several major merits: the sticky adhesive tape can seal the microfluidic structure easily, avoiding the bonding process; the immobilization is easy and environmental friendly, without the need for expensive reagents or complex processes; the adhesive tape substrate allows the flexibility of microfluidic chips; and the adhesive tape substrate can be stripped off for off-chip detection and can be replaced easily for the reuse of microfluidic structures. With these, the biomimetic method may find potential applications in environmental sensing, biocatalysis and biosynthesis using microchips.

1. Introduction

Microfluidics presents great potential for high-throughput biological/chemical detection, catalysis and synthesis due to its inherent advantages, such as large surface-area-to-volume ratio, fast reaction rate, high-precision manipulation and easy flow control [1–5]. The corresponding detection–promoting substances catalysts or carriers are mostly nanoparticles or nanoparticle-involved compounds [6,7]. Actually, nanoparticles are highly preferred to be immobilized on the substrates since their separation and recycling from a mixture are laborious and troublesome [8]. Based on the working principles, the immobilization techniques can be broadly divided into four categories: magnetic attraction, covalent binding, polymer entrapment and surface adsorption. The first three methods function well, but mostly require complicated processes, expensive reagents/equipment, and even harmful chemicals. The surface adsorption method is simple and environmentally friendly, but the adsorption amount is disappointing and the bond strength is often too weak to resist the high shear stress caused by the laminar flow in microfluidic devices.

Our mother nature has already evolved a highly efficient model of particle immobilization, i.e., the feeding system of clams (as shown in Fig. 1A). In this system, water and food particles (e.g. the phytoplankton) are drawn in through the incurrent siphon, in which the hair-like cilia move the water to the gills. Then, food particles are caught in mucus (sticky fluid) produced by the gills [9]. In this process, mucus plays a very important role in the efficient food particle capture process (Fig. 1B). To simply mimic such an efficient model for nanoparticle immobilization, we propose to use a common adhesive tape as the microfluidic chip substrate, which has sticky polyacrylate surface with surface charges and radicals. Actually, the common adhesive tape has contributed to the Nobel-winning work on graphene [10], triboluminescence [11] and the reduction of metal salts to the corresponding metal nanoparticles [12]. Moreover, other different kinds of tapes, such as double sided adhesive tapes and adhesive transfer tapes have been used in microfluidics for various functions, such as rapid prototyping and PCR [13–15]. The acrylic pressure-sensitive adhesive is typically a "pure polymer" composition (e.g., polyacrylates, the average

* Corresponding author at: The Hong Kong Polytechnic University Shenzhen Research Institute, Shenzhen, PR China.
E-mail address: apzhang@polyu.edu.hk (X. Zhang).

http://dx.doi.org/10.1016/j.snb.2015.08.069

molecular weight from 100,000 to 1,000,000–5,000,000) [16], it can produce adhesion by itself. It is reasonable to expect the nanoparticles to be trapped by the adhesion force, or more specifically, van der Waal's force. This is the same mechanism as what the mucus of clams uses to capture the floating particles [17]. In contrast, the glass slide is traditionally a common substrate for particle immobilization, but often needs complicated surface modifications to anchor linker molecules containing organic groups like amine and thiol, especially when Au nanoparticles are to be trapped [18,19]. In this sense, the adhesive tape substrate is favorable as it avoids the need for surface modifications and expensive reagents.

This biomimetic device presents many advantages. First, the upper layer of microfluidic chip (usually made of polydimethylsiloxane, PDMS) can be sealed by simply pressing it against the adhesive tape, without the use of plasma bonding. The adhesive bond is temporary but strong enough to resist a high flow rate. Second, the adhesive tape can be easily stripped off from the PDMS structure for off-chip detection and can be replaced by a new adhesive tape to reuse the microfabricated PDMS layer, making the device portable, repeatable and inexpensive. Third, similar to the mucus-covered feeding structures, the adhesive tapes immobilize nanoparticles easily and efficiently. Fourth, the combination of PDMS and adhesive tape allows the microfluidic chip to be soft and flexible. In this work, we will experimentally study the immobilization properties of nanoparticles by the adhesive tape substrate and will further investigate the surface-enhanced Raman scattering (SERS) detection of rhodamine 6G (R6G) using the immobilized Au nanoparticles, with the aim to demonstrate the potential for biochemical sensing applications.

2. Materials and methods

The PDMS layer (width 1 mm and height 40 μm) with a simple pattern of serpentine microchannel was fabricated using standard soft lithography techniques (see Fig. 1C) [20]. Different from the normal plasma bonding process on a glass substrate, the PDMS layer was sealed directly by pressing it onto the transparent adhesive tape (3 M Company), without the use of plasma cleaners. As the tape has tacky substance on the surface, it can be adhered to another surface by applying a light pressure. The recommended bonding pressure is 14.5–29 psi (i.e., 100–200 kPa). Optical images show that the fabricated microfluidic chips are still transparent. Liquid with blue color is flowed along the microchannel smoothly and the flexibility of these chips is good (see Fig. 1D and the inset).

The bond strength between the PDMS and the adhesive tape substrate was characterized by two methods, *channel deformation test* and *direct interface bond strength test* using a digital force gauge (Aigu, Hong Kong). In the first test, the flow injected into the microchannel was slowly increased until a clear channel deformation was observed, and this flow rate was recorded as the critical flow rate. Here, we consider the channel deformation as an important factor but not the leakage since the stability of channel shape is important to many microfluidic applications, such as droplets, bubbles and laminar flow formation [21–25]. In the second test, a PDMS layer (5 mm × 5 mm) adhered to a transparent adhesive tape was pulled by a digital force gauge. With the increase of the tension offered by the force gauge, the PDMS layer was separated from the adhesive tape. This force read from the gauge is the bond strength between the PDMS and the adhesive tape substrate. Each test was repeated for five times.

The immobilization stage was processed by the introduction of TiO_2 nanoparticle–water or TiO_2 nanoparticle–ethanol suspension into the microfluidic channels (50 mg/mL). The TiO_2 nanoparticles were P25 from Sigma–Aldrich, with the average size of 21 nm. During this immobilization process, the adhesive tapes trapped the TiO_2 nanoparticles tightly. To assess the immobilization effect, we compared the immobilization density on the adhesive tape with that on the glass slide using the same method. To investigate the adhesion strength of nanoparticles, we performed a shear stress test by flushing the microchannel at the critical pressure for ten minutes. During this test, we captured the optical images once every minute, followed by the calculation of TiO_2 nanoparticle

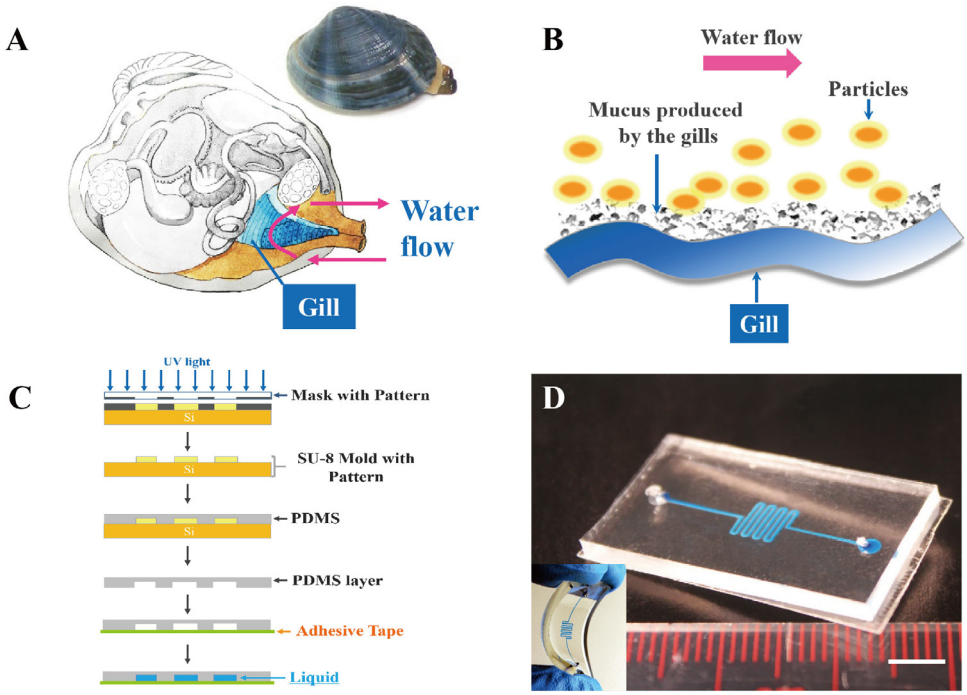

Fig. 1. Nanoparticle immobilization of the adhesive tape substrate by mimicking the clam. (A) Clam internal anatomic diagram. (B) Capture of floating particles by the gill secreted mucus. (C) Process flow of the PDMS microfluidic device using soft lithography. (D) Optical image of the fabricated microfluidic chips. PDMS layer was sealed simply pressing against the adhesive tape, without the need for the bonding process by plasma cleaners. The inset illustrates the flexibility of this chip. The scale bar is 5 mm.

densities before and after the test using the software Image-Pro Plus 6. To explore more functions, we immobilized Au nanorods for SERS detection. The synthesis of the Au nanorods followed the previous seed-mediated method [26,27] and the as-prepared Au nanorods were precipitated, washed and redispersed in water (10 mL). Here, the zeta potential of the nanoparticles is $+31.0 \pm 1.0$ mV, as by measured by the particle sizer (Zetasizer 3000 HSa, Malvern). A mixture of 10 μL Au nanorods suspension and 10 μL rhodamine 6G (R6G, Sigma-Aldrich) (1×10^{-4} M) were premixed and incubated for 10 min at room temperature, followed by the manual injection into the microchannel and then the incubation for another 20 min. During this process, the Au nanorods absorbed with R6G were immobilized on the microchannel substrate. Nevertheless, the glass slide without the modification like thiol is hard to immobilize the Au nanorods, and thus the SERS detection of R6G has low sensitivity and is inaccurate.

The prepared Au nanorods were drop-cast on a TEM grid to perform high-resolution morphology characterization and EDX element mapping using a JEM2100F TEM system operating at 300 kV. The extinction spectra of the metal nanorods were obtained on a UV–vis absorption spectrometer (Shimadzu Scientific Instruments, UV2550). The Raman spectra of the solution were recorded using a Raman spectrometer from Princeton Instruments (Horiba HR800) with an excitation laser of 633 nm. The laser power was approximately 1 mW. Through an aperture of 100 μm in diameter, the laser was focused onto a ca. 0.3 μm diameter spot on the sample surface via a long working distance 100 × objective. The integration time was set at 5 s, and the spectral range was from 1000 to 1800 cm^{-1}.

In the above immobilization tests, the as-synthesized Au nanoparticles are positively charged, whereas the TiO_2 nanoparticles are not charged (i.e., having high surface energy). For comparison and also for the study of adhesion mechanisms, we further tested polystyrene nanospheres, which is neutral but hydrophobic (having a low surface energy) [28]. Two types of polystyrene nanospheres (ϕ5 μm without fluorescence and ϕ0.39 μm with orange fluorescence) were procured from Duke Scientific Corp. The excitation wavelength is 542 nm and the emission is 612 nm.

3. Results and discussion

3.1. Fabricated microfluidic chips

For experimental study, we fabricated microfluidic chips using the adhesive tape as the substrate for nanoparticle immobilization and proved the stability, high efficiency and detection ability of this immobilization method. The preparation of the PDMS microfluidic device was shown in Fig. 1C. And the adhesive tape offers a good sealing of the PDMS microstructure as shown in Fig. 1D. Notably, the thickness of the microfluidic chip with the adhesive tape substrate is much thinner than that with a glass substrate because the adhesive tape is only 22 μm thick. Also, this adhesive tape substrate makes the microfluidic chip flexible, which the glass substrate lacks. In the inset graph of Fig. 1D, we show the flexibility of the as-prepared chip by bending it but without disrupting the microchannel structure or function. This flexibility feature holds great potential for wearable electronics, health monitoring, point-of-care diagnostics, environmental sensing and many other applications [29].

3.2. Test of bond strength

Various methods have been developed to test the bond strength, such as peel test, scratch test, pull test and blister test [30]. For the peel test, the sample preparation is typically simple and gives a semi-quantitative measure of the test layer to the substrate, but it is difficult to initiate a peel strip if the test layer is strongly adhered to the substrate. Similarly, the sample preparation of the scratch test is relative easy, but this method is limited to hard brittle coatings. On the other hand, the pull test is suitable for almost all types of test layers; however, the test should be repeated for several times to get reliable quantitative data. In contrast, the blister test is a fully quantitative analysis but requires a complicate preparation of the functional device. Thanks to the easily repeatable nature and the functional diversity of the microfluidic chips, here we choose the blister test and the pull test to detect the bond strength between the PDMS and the tape substrate. The first one is the channel deformation test, which essentially belongs to the blister test. In the initial state, the optical image of the microchannel is shown in Fig. 2A. With the increase of the flow rate, the microchannel is deformed gradually and some bubble-like defects are developed slowly. For instance, up to 200 μL/min, the defect is still small as shown in Fig. S1. When the flow rate reaches 225 μL/min and goes beyond, the size of defects begins to increase rapidly (see the blue arrows in Fig. 2B and more discussions in ESI session S1). And this critical flow rate, 225 μL/min, reflects the bond strength between the PDMS layer and the adhesive tape substrate. Actually, it is favorable to use the critical flow rate as the bond strength indicator. First, the flow rate is a basic parameter of the microfluidic systems, providing a straightforward operation parameter. In addition, the flow rate can be precisely controlled by a syringe pump. By setting the flow rate below the critical one, it is easy to avoid the deformation, leakage and breakage of the microfluidic system. However, the flow rate is not enough to directly quantify the bond strength. Therefore, a standard pull test (i.e., a direct interface bond strength test) using a digital force gauge is conducted. When the tension of the force gauge was increased gradually, the PDMS layer was separated from the adhesive tape. It is measured that the bond strength between the PDMS and the adhesive tape substrate is ~0.2099 N/mm^2 (equivalent to 210 kPa), and this test has been repeated for five times. Although the bond strength between the PDMS layer and the adhesive tape substrate is weaker than the traditional plasma method, the critical flow rate and the bond strength in this method are high enough for many microfluidic applications.

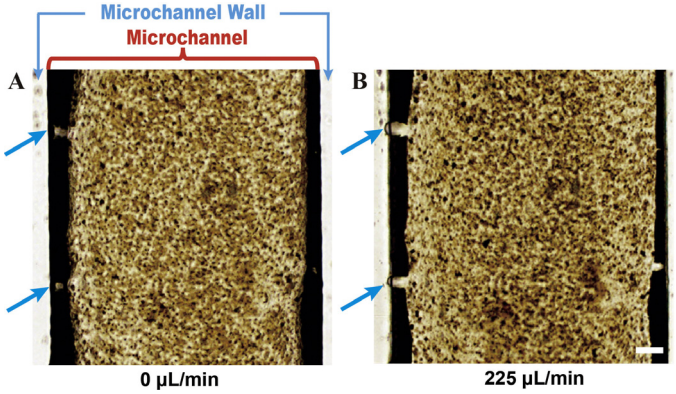

Fig. 2. Immobilization of TiO_2 nanoparticles and test of bond strength. (A) Optical image of the immobilized TiO_2 on the adhesive tape substrate after the drying process and the slow refilling of water (the initial state, also named as 0 μL/min). (B) Parts of the microchannel (pointed by the blue arrows) start to deform when the flow rate is gradually increased to 225 μL/min, indicating the maximum bearable flow rate. The scale bar is 100 μm. (For interpretation of the references to color in this figure legend, the reader is referred to the web version of this article.)

3.3. Immobilization of TiO_2 nanoparticles

The immobilization of nanoparticles is easy to operate. The TiO_2 nanoparticle–water suspension was introduced into the

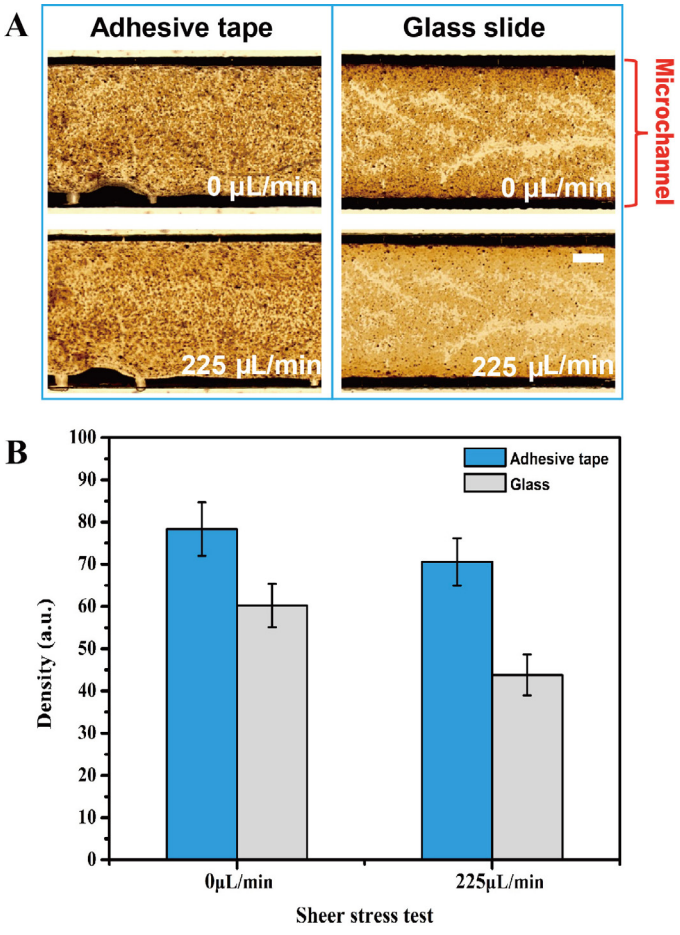

Fig. 3. Shear stress tests of the immobilized TiO_2 nanoparticles. (A) Optical images of the immobilized TiO_2 nanoparticles on the adhesive tape substrate and the glass substrate before and after applying a flow rate of 225 μL/min for ten minutes. (B) Particle densities of the optical images. After flushing, the glass substrate loses more nanoparticles than that on the adhesive tape substrate. The scale bar is 200 μm.

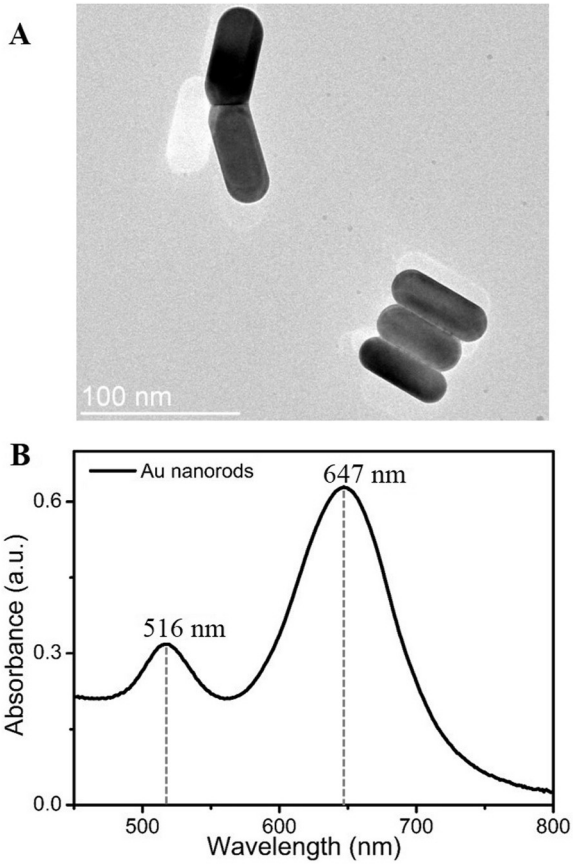

Fig. 4. (A) High resolution TEM images of the Au nanorods of single crystal lattice. (B) UV–vis absorption spectra of the Au nanorods.

microchannel and became ready to use once the liquid was dried by the evaporation through the PDMS layer. To prove that the organic solution is also applicable for this acrylate-made adhesive tape, we tried ethanol as the solution as well. In fact, ethanol has much faster evaporation rate than the water. On average, this process only takes 10 min to get a good result as shown in Fig. 2A. Unavoidably, there are small void regions in the substrate because of the aggregation of TiO_2 nanoparticles during the drying process.

The particle densities on the adhesive tape substrate and the glass substrate are shown in Fig. 3A. It can be seen that after drying the nanoparticle solutions in the microfluidic channels and then slowly refilling the microchannels with water (we define this state as the flow rate 0 μL/min), the nanoparticles on the adhesive tape substrate (Fig. 3A, upper left) are denser and more uniform than those on the glass substrate (Fig. 3A, upper right). As described above, the microfluidic chips of both types of substrates were then flushed at 225 μL/min for 10 min, and the optical images were captured once every minute. Here, the corresponding shear stress τ could be calculated from the flow rate Q and the microchannel geometry based on the equation [31]: $\tau = 6\eta Q/h^2 w$ where h is the channel height, w the channel width and η the viscosity of fluid. In this work, h is 40 μm, w is 1000 μm and η is 0.001 Pa s (20 °C). Thus, the shear stress for 225 μL/min is 563 Pa. In experiment, we found an obvious drop of particle density from 0 to 1 min, caused by the loss of nanoparticles that were bound loosely, but only a slight change from 2 min to 10 min. Thus, we only used the data after the first minute to evaluate the immobilization effect. From the images in the lower row of Fig. 3A, it can be seen that the adhesive tape substrate retains more nanoparticles than the glass substrate. From the data columns in Fig. 3B, the particle density of the adhesive tape substrate is close to that of the glass substrate in the initial state, but becomes 1.43 times more after the flushing. This well shows that the adhesive tape substrate is effective on the nanoparticle immobilization and can sustain high shear stress.

3.4. Immobilization of Au nanorods for SERS detection

As a demonstration of the potential applications, we used the adhesive tape substrate to immobilize Au nanorods for the SERS detection of R6G. Fig. 4A shows the high resolution TEM image of the as-prepared Au nanorods, which are ~60 nm in length and ~20 nm in diameter. The absorption spectrum of these Au nanorods is plotted in Fig. 4B, showing two absorption peaks at 515 nm and 647 nm owing to the transverse and longitudinal localized surface plasmon resonances. The Au nanorods were premixed with R6G before being injected into the microchannels. The SERS detection was sampled near the inlet because the density of Au nanorods immobilized onto the adhesive tape substrate decreases along the flowing direction [32].

The curve group (1) in Fig. 5A plots the SERS–RSD spectra of R6G molecules (concentration 5×10^{-6} M) collected from six randomly-selected locations of the substrate near the inlet. The major SERS peaks are clear and coherent with the reported studies [33,34]. The Raman shifts at 1206, 1319, 1369 and 1516 cm^{-1} are associated with the characteristic vibrational modes of a C—H band and an

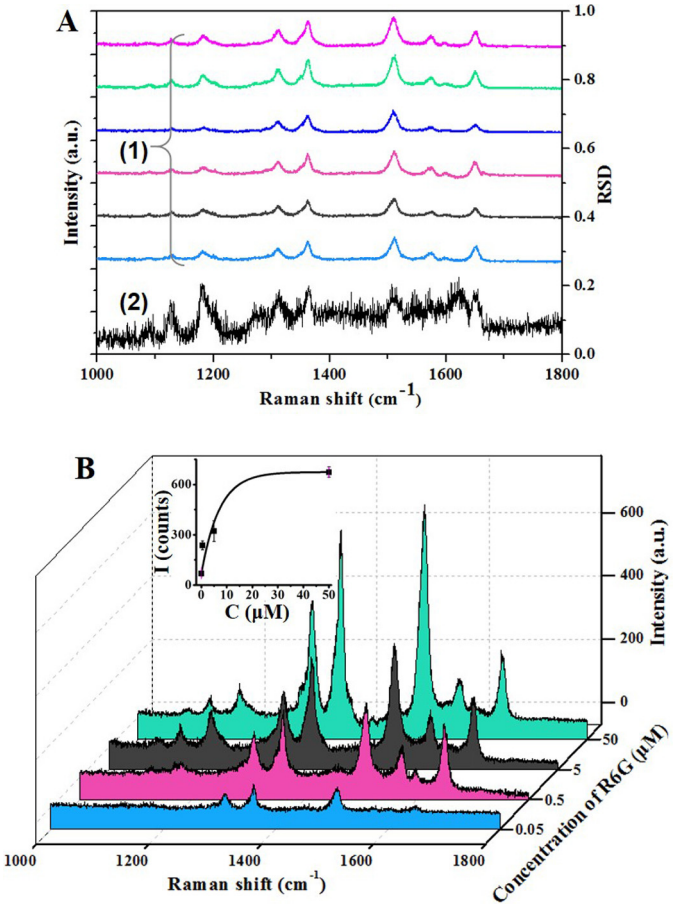

Fig. 5. (A) SERS spectra of R6G molecules (5×10^{-6} M) collected from six arbitrary locations of the adhesive tape substrate within the microfluidic channel (curve group 1) and the corresponding RSD curve (curve 2). (B) SERS spectra for different concentrations of R6G. The inset plots the intensity of 1507 cm^{-1} peak versus the concentration.

aromatic C—C stretching band of R6G, respectively. Curve (2) of Fig. 5A plots the relative standard deviation (RSD) of the spectral data, and the RSD value was below 0.2, indicating the immobilized Au nanorods achieved reliable active sites for the sample detection. Then, we detected different concentrations of R6G (0.05 μM, 0.5 μM, 5 μM and 50 μM) using the same method. As can be seen from Fig. 5B, the intensity of peaks goes up with the increase of R6G concentration. The inset plots the intensity of 1507 cm^{-1} Raman shift peak as a function of the concentration. Each data point is an average of five measurements at five different locations. The peak intensity tends to saturate for high concentration level, and the concentration of 50 μM R6G is nearly the maximum that can be absorbed by the Au nanorods in the microfluidic chip.

3.5. Mechanism of adhesion

Over the past decades, different theories have been proposed for the mechanism of adhesion, such as mechanical theory, electrostatic theory and adsorption theory [28]. The mechanical theory is based on the mechanical anchorage of the adhesive by pores and irregularities. The electrostatic theory is based on the formation of an electric double layer at the adhesive–adherent boundary and the corresponding Coulomb attraction forces between the two parts. Differently, the forces that are responsible for the adsorption theory are the van der Waals' forces, including three components, namely, the Keesom's dipole orienting effect, the Debye's induced dipole effect, and the London's dispersion effect. So the entirely thermodynamic principles are the basis of this theory and the surface energy of the adhesive must be lower than that of the adherent for adhesion. For example, metals with a high surface energy and paper with a medium surface energy can be bonded easily to the adhesive; whereas some polymers (e.g. polystyrene) having a low surface energy are difficult for bonding.

In our cases, all these three theories should be used to explain the adhesion of different nanoparticles. The mechanical theory works on most types of particles since the sticky layer of the adhesive tape is a porous structure. However, if the particles have positive or negative charges, the electrostatic theory comes into play since the sticky side of the adhesive tape forming positive and negative charged species upon peeling [12]. In our experiment, the zeta potential of the Au nanorods is $+31.0 \pm 1.0$ mV, the electrostatic attraction between the positive Au nanorods and the negative charged species plays the major role in the adhesion. In terms of the neutral particles (e.g., TiO_2 nanoparticles), the adhesion can be attributed to the van der Waals' force in the adsorption theory. To prove this point, we tried with two types of polystyrene nanospheres suspended in water, and found that very few polystyrene nanospheres could be immobilized onto the adhesive tapes after the evaporation of water (see details in ESI session S2). The efficient trapping of TiO_2 nanoparticles and the failing trapping of polystyrene nanoparticles can be easily explained by the adsorption theory, because the hydrophilic TiO_2 nanoparticles have high surface energy and the hydrophobic polystyrene nanoparticles have very low surface energy.

The above results of the bond strength test, the shear stress test and the SERS detection, have showed that this method is superior in many aspects. However, this adhesive tape still has its limitations. For instance, the adhesive tape is a common type, with low chemical resistance and low temperature stability. And the bond between the PDMS layer and the adhesive tape is weaker than the traditional plasma method. Since the focus of this paper is to present a new approach, rather than a method to replace all existed methods, shortcomings and limitations will be improved in future work.

4. Conclusions

We proposed a novel biomimetic method to immobilize nanoparticles by using adhesive tape as the microfluidic substrate. It was inspired by the mucus-covered feeding system of the clams. After the bond strength test, the shear stress test and the SERS detection, we found this method simple and effective. The bond strength between PDMS and the common adhesive tape reaches 210 kPa and is able to resist a flow rate of 225 μL/min, high enough for many microfluidic applications. We observed that TiO_2 nanoparticles immobilized on the adhesive tape substrate are denser than those on the glass substrate and showed a stronger resistance to the shear stress. Moreover, we immobilized Au nanorods for the detection of R6G in various concentrations, demonstrating its usefulness for biochemical sensing applications. This immobilization method with simple, cheap and replaceable nature may find applications in various fields, especially detections, biocatalyses and biosyntheses.

Acknowledgements

This work is partially supported by The Research Grants Council (RGC) of Hong Kong through the General Research Fund (PolyU 5334/12E and N_PolyU505/13), The Hong Kong Polytechnic University (4-BCAL, G-YN07, G-YBBE, 1-ZE14 and 1-ZVAW) and National Science Foundation of China (No. 61377068).

Appendix A. Supplementary data

Supplementary data associated with this article can be found, in the online version, at http://dx.doi.org/10.1016/j.snb.2015.08.069.

References

[1] G.M. Whitesides, The origins and the future of microfluidics, Nature 442 (2006) 368–373.
[2] N. Wang, X. Zhang, B. Chen, W. Song, N.Y. Chan, H.L.W. Chan, Microfluidic photoelectrocatalytic reactors for water purification with an integrated visible-light source, Lab Chip 12 (2012) 3983–3990.
[3] N. Wang, X. Zhang, Y. Wang, W. Yu, H.L.W. Chan, Microfluidic reactors for photocatalytic water purification, Lab Chip 14 (2014) 1074–1082.
[4] R. Gorkin, J. Park, J. Siegrist, M. Amasia, B.S. Lee, J.M. Park, et al., Centrifugal microfluidics for biomedical applications, Lab Chip 10 (2010) 1758–1773.
[5] C. Zhao, Y. Xie, Z. Mao, Y. Zhao, J. Rufo, S. Yang, et al., Theory and experiment on particle trapping and manipulation via optothermally generated bubbles, Lab Chip 14 (2014) 384–391.
[6] C. Hu, W. Yue, M. Yang, Nanoparticle-based signal generation and amplification in microfluidic devices for bioanalysis, Analyst 138 (2013) 6709–6720.
[7] W.J. Duncanson, T. Lin, A.R. Abate, S. Seiffert, R.K. Shah, D.A. Weitz, Microfluidic synthesis of advanced microparticles for encapsulation and controlled release, Lab Chip 12 (2012) 2135.
[8] Z. Meng, X. Zhang, J. Qin, A high efficiency microfluidic-based photocatalytic microreactor using electrospun nanofibrous TiO_2 as a photocatalyst, Nanoscale 5 (2013) 4687–4690.
[9] S.G. Hinch, L.A. Stephenson, Size- and age-specific patterns of trace metal concentrations in freshwater clams from an acid-sensitive and a circumneutral lake, Can. J. Zool. 65 (1987) 2436–2442.
[10] K.S. Novoselov, A.K. Geim, S.V. Morozov, D. Jiang, Y. Zhang, S.V. Dubonos, et al., Electric field effect in atomically thin carbon films, Science 306 (2004) 666–669.
[11] C.G. Camara, J.V. Escobar, J.R. Hird, S.J. Putterman, Correlation between nanosecond X-ray flashes and stick–slip friction in peeling tape, Nature 455 (2008) 1089–1092.
[12] H.T. Baytekin, B. Baytekin, S. Huda, Z. Yavuz, B.A. Grzybowski, Mechanochemical activation and patterning of an adhesive surface toward nanoparticle deposition, J. Am. Chem. Soc. 137 (2015) 1726–1729.
[13] J. Kim, R. Surapaneni, B.K. Gale, Rapid prototyping of microfluidic systems using a PDMS/polymer tape composite, Lab Chip 9 (2009) 1290–1293.
[14] P. Nath, D. Fung, Y.A. Kunde, A. Zeytun, B. Branch, G. Goddard, Rapid prototyping of robust and versatile microfluidic components using adhesive transfer tapes, Lab Chip 10 (2010) 2286–2291.
[15] A.W. Martinez, S.T. Phillips, G.M. Whitesides, Three-dimensional microfluidic devices fabricated in layered paper and tape, Proc. Natl. Acad. Sci. U. S. A. 105 (2008) 19606–19611.
[16] C.W. Taylor, Packaged, sterilized, pressure sensitive adhesive products, CN1161053 A.
[17] X. Yu, H. Liu, Y. Yang, S. Lu, Q. Yao, P. Yi, The investigation of the interaction between oxymetazoline hydrochloride and mucin by spectroscopic approaches, Spectrochim. Acta – Part A Mol. Biomol. Spectrosc. 103 (2013) 125–129.
[18] T. Okamoto, I. Yamaguchi, T. Kobayashi, Local plasmon sensor with gold colloid monolayers deposited upon glass substrates, Opt. Lett. 25 (2000) 372–374.
[19] H. Weinrib, A. Meiri, H. Duadi, D. Fixler, Uniformly immobilizing gold nanorods on a glass substrate, J. Phys. B: At. Mol. Opt. Phys. 2012 (2012) 1–6.
[20] D.C. Duffy, J.C. McDonald, O.J.A. Schueller, G.M. Whitesides, Rapid prototyping of microfluidic systems in poly(dimethylsiloxane), Anal. Chem. 70 (1998) 4974–4984.
[21] P. Garstecki, M.J. Fuerstman, H.A. Stone, G.M. Whitesides, Formation of droplets and bubbles in a microfluidic T-junction-scaling and mechanism of break-up, Lab Chip 6 (2006) 437–446.
[22] X. Huang, W. Hui, C. Hao, W. Yue, M. Yang, Y. Cui, et al., On-site formation of emulsions by controlled air plugs, Small 10 (2014) 758–765.
[23] X. Huang, L. Li, Q. Tu, J. Wang, W. Liu, X. Wang, et al., On-chip cell migration assay for quantifying the effect of ethanol on MCF-7 human breast cancer cells, Microfluid. Nanofluid. 10 (2011) 1333–1341.
[24] D. Bardin, A. Lee, Low-cost experimentation for the study of droplet microfluidics, Lab Chip 14 (2014) 3978–3986.
[25] J.Q. Yu, W. Huang, L.K. Chin, L. Lei, Z.P. Lin, W. Ser, et al., Droplet optofluidic imaging for λ-bacteriophage detection via co-culture with host cell *Escherichia coli*, Lab Chip 14 (2014) 3519–3524.
[26] Z.Y. Bao, D.Y. Lei, R. Jiang, X. Liu, J. Dai, J. Wang, et al., Bifunctional Au@Pt core–shell nanostructures for in situ monitoring of catalytic reactions by surface-enhanced Raman scattering spectroscopy, Nanoscale 6 (2014) 9063–9070.
[27] W. Ni, X. Kou, Z. Yang, J. Wang, Tailoring longitudinal surface plasmon wavelengths, scattering and absorption cross sections of gold nanorods, ACS Nano 2 (2008) 677–686.
[28] W.K. Gerhard Gierenz, Adhesives, in: Adhesives and Adhesive Tapes, Wiley-VCH, New York, 2001.
[29] B. Zhang, Q. Dong, C.E. Korman, Z. Li, M.E. Zaghloul, Flexible packaging of solid-state integrated circuit chips with elastomeric microfluidics, Sci. Rep. 3 (2013) 1098.
[30] R. Lacombe, Adhesion Measurement Methods: Theory and Practice, CRC Press, Boca Raton, 2006.
[31] R. Sun, S. Muller, J. Stoltz, X. Wang, Shear stress induces caveolin-1 translocation in cultured endothelial cells, Eur. Biophys. J. 30 (2002) 605–611.
[32] Y. Guo, M.K. Khaing Oo, K. Reddy, X. Fan, Ultrasensitive optofluidic surface-enhanced Raman scattering detection, ACS Nano 6 (2012) 381–388.
[33] P. Hildebrandt, M. Stockburger, Surface-enhanced resonance Raman spectroscopy of Rhodamine 6G adsorbed on colloidal silver, J. Phys. Chem. 88 (1984) 5935–5944.
[34] S. Yang, P.J. Hricko, P.H. Huang, S. Li, Y. Zhao, Y. Xie, et al., Superhydrophobic surface enhanced Raman scattering sensing using Janus particle arrays realized by site-specific electrochemical growth, J. Mater. Chem. C 2 (2014) 542–547.

Biographies

Xiaowen Huang is currently pursuing her Ph.D. degree in the Department of Applied Physics, The Hong Kong Polytechnic University (PolyU), Hong Kong. She received her M.S. in Cell Biology at Northwest A&F University, Shaanxi, China, in 2011. Her current research interest is focused on the fabrication of microfluidic chips as a fast and simple screening detection platform for food contamination and water pollution.

Yujiao Zhu is currently a M.Phil. candidate in The Hong Kong Polytechnic University. She received her bachelor's degree in School of Materials Science and Engineering in the University of Science and Technology Beijing in 2014. Her research interest is bio-microfluidics and nanomaterials.

Xuming Zhang received B.E. degree in Mechanical Engineering from University of Science & Technology of China (USTC) in 1994, two M.E. degrees in 1997 and 2000, respectively. Finally, he got Ph.D. degree from Nanyang Technological University (NTU) in Electrical & Electronic Engineering in 2006. He took up an associate professor position in 2015 in Department of Applied Physics, Hong Kong Polytechnic University. His research focuses mainly on microfluidics, photocatalysis, fiber sensors and nanophotonics.

Zhiyong Bao, as a Ph.D. candidate, studies in Department of Applied Physics, The Hong Kong Polytechnic University. His research interests include functional nanomaterials and SERS.

Dangyuan Lei is an assistant professor in Department of Applied Physics, The Hong Kong Polytechnic University. He received his Ph.D. degree from Imperial College London. He focuses on nanophotonics and nanomaterials (including 2D materials) studies, with particular interest in surface plasmon-enhanced light-matter interactions at the nanoscale and their applications in energy harvesting, optoelectronic devices, biochemical sensing and biomedical imaging.

Weixing Yu received his B.Sc. from Northwestern Polytechnical University, Xi'an, China, in 1998, M.Sc. from Changchun Institute of Optics, Fine Mechanics and Physics (CIOMP), Changchun, China, in 2001 and Ph.D. from Nanyang Technological University, Singapore in 2005. Before he joined CIOMP, he worked in Advanced Packaging Solutions Ltd (Singapore), Schott (Shanghai) and MIcroSystems Engineering Centre (MISEC) of Heriot–Watt University (UK) as a Senior Engineer, Research Scientist and Postdoctoral Research Associate respectively. He is now working in CIOMP as a young distinguished scholar under the scheme of "Hundred Talents Program". His research interests are in micro/nanooptics, micro/nanofabrication and microelectronics packaging.

Jiyan Dai received his B.Sc. degree in physics from Fudan University in 1988, his M.S. degree in electrical engineering from Tsinghua University in 1991, and his Ph.D. degree in materials physics from the Chinese Academy of Sciences in 1994. He has worked at Northwestern University as a Research Associate for three years, and after one year working in the Institute of Materials Research and Engineering Singapore, he joined Chartered Semiconductor Manufacturing Ltd. in Singapore in failure analysis. His research interest is materials science and medical ultrasound transducers. He joined the Department of Applied Physics at the Polytechnic University in 2001 as lecturer and currently is Associate Professor. He has been working on a few projects in fabricating endoscopic and high-frequency ultrasound transducers and imaging systems.

Yu Wang received his B.Sc., M.Sc. and Ph.D. degrees in Tsinghua University, China. Now his is an associate professor in Department of Applied Physics, Hong Kong Polytechnic University. His research interests are ferroelectric thin films, single crystals and detection.